Photoabsorption spectra of Ti_8C_{12} metallocarbohedrynes: Theoretical spectroscopy within time-dependent density functional theory

J. I. Martinez[a)]
Departamento de Fisica Teórica, Atómica y Optica, Universidad de Valladolid, 47001 Valladolid, Spain; Institut für Theoretische Physik, Freie Universität Berlin, 14195 Berlin, Germany; and Donostia International Physics Center (DIPC), 20018 San Sebastian, Spain

A. Castro
Institut für Theoretische Physik, Freie Universität Berlin, 14195 Berlin, Germany

A. Rubio
Institut für Theoretische Physik, Freie Universität Berlin, 14195 Berlin, Germany; Donostia International Physics Center (DIPC), 20018 San Sebastian, Spain; Departamento de Física de Materiales, Facultad de Químicas, Universidad del País Vasco and Centro Mixto CSIC-UPV/EHU, 20080 San Sebastián, Spain; and European Theoretical Spectroscopy Facility, Donostia International Physics Center (DIPC), 20018 San Sebastian, Spain

J. A. Alonso
Departamento de Fisica Teórica, Atómica y Optica, Universidad de Valladolid, 47001 Valladolid, Spain and Donostia International Physics Center (DIPC), 20018 San Sebastian, Spain

(Received 17 May 2006; accepted 10 July 2006; published online 21 August 2006)

The photoabsorption spectra of several of the most stable isomers of the Ti_8C_{12} metallocarbohedryne are calculated using time-dependent density functional theory. Several ground-state magnitudes have been also calculated, such as cohesive energies, electronic gaps between the highest occupied and lowest unoccupied molecular orbitals, and static polarizabilities. Since significant differences are found among the photoabsorption spectra of the different isomers in the low energy region (0–5 eV), we propose the comparison of experimental and the calculated absorption spectra as a tool to elucidate the isomers that appear to form in the experiments. Between 10 and 13 eV all the spectra show a region of high absorption that we identify as due to collective electronic excitations. The existence of this prominent feature explains the occurrence of delayed ionization and delayed ion emission phenomena observed in previous experiments. © *2006 American Institute of Physics*. [DOI: 10.1063/1.2263732]

I. INTRODUCTION

Metallocarbohedrynes—or met-cars, for short—are a class of stable and highly symmetric clusters discovered in 1992 by Guo *et al.*[1] These clusters were obtained using a laser vaporization source to induce the reaction between transition-metal atoms and hydrocarbons. The met-car family comprises species with the stoichiometric formula M_8C_{12}, where M is an early transition metal mainly (Ti, V, Zr, Nb, Hf, Mo, Cr, and Fe).[2,3] In contrast to other metal-carbon clusters, metallocarbohedrynes also exhibit multicage growth patterns,[4] M_nC_m with $[n,m]=[13,22]$, [14, 21], [18, 29], and [22, 35]. Species containing combinations of two metals, such as $Ti_{8-x}M_xC_{12}$, have also been detected.[5] Other exciting properties of these clusters are a relatively low ionization potential, the occurrence of delayed ionization and ion emission,[6] an active behavior as hydrodesulfurization catalyst;[7] and a potentially interesting magnetic behavior due to the presence of transition metal elements. In particular, an appealing feature is the role that the d electrons of the transition metal atoms play in the stability of the cluster. The met-cars are expected to exhibit rich chemical and physical properties that may find applications in electronics and catalysis. A review on the subject may be found in Ref. 8.

The geometrical structure of the met-cars has generated a lot of debate. Early studies proposed for the structure of Ti_8C_{12} and V_8C_{12} a pentagonal dodecahedral cage of T_h symmetry. This proposal was motivated by the reaction behavior with NH_3, and by ligand titration experiments, which suggested that the eight metal atoms had similar coordination.[2] Later, different authors have proposed alternative configurations based on density functional calculations.[9] Dance proposed a tetracapped tetrahedron of T_d symmetry as the ground state, showing that the T_h dodecahedral structure was higher in energy by 15 eV.[10,11] Other optimized geometries have been suggested, belonging to the D_{2d} point group.[12] In several papers, Rohmer *et al.* have suggested seven structures as local minima on the potential-energy surface of Ti_8C_{12}.[8,13,14] Soon after, Gueorguiev and Pacheco,[15] in addition to calculating the infrared-absorption spectrum of Ti_8C_{12}, found that a Jahn-Teller distorted T_d geometry was the lowest-energy configuration. The most recent calculations have proposed for the met-cars a C_{3v} structure[16–19] rather similar to the distorted T_d structure. Studies of neutral,

a)Electronic mail: nacho@lab2.fam.cie.uva.es

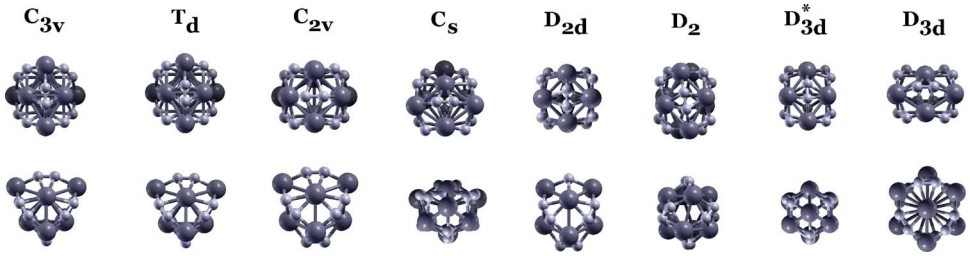

FIG. 1. (Color online) Top and side views (upper and lower rows, respectively) of the isomeric Ti_8C_{12} structures, belonging to the C_{2v}, C_{3v}, C_s, D_2, D_{2d}, D_{3d}, D^*_{3d}, and T_d symmetry groups, used for the calculation of the photoabsorption spectra. Relative energies are given in Table I. Large and small spheres represent Ti and C atoms, respectively.

cationic, and anionic Ti_8C_{12} clusters with C_{3v}, D_{2d}, and T_d structures by Deng *et al.*[20] reveal that the most stable geometry depends strongly on the charge state.

The assignment of the equilibrium geometry of the neutral titanium met-car as a C_{3v} structure appears to be a trustable conclusion of the theoretical calculations, although this assignment awaits confirmation from experiments. One of the experimental methods that can be used is photoabsorption spectroscopy. For this reason the objective of this paper is to calculate the photoabsorption spectrum of a number of low lying isomers of Ti_8C_{12} with the structures taken from the recent work of Sobhy *et al.*[19] For this purpose we use the time-dependent density functional theory (TDDFT).[21] In fact, we have proposed in previous papers[22,23] that a comparison of the measured optical spectrum with calculations of the spectra for different isomeric forms of a given cluster can provide a useful diagnosis of its geometrical structure. We show here that the differences found among the photoabsorption spectra of the different isomers in the low energy region (0–5 eV) can be used as a convenient tool to distinguish the different met-car isomers.

In addition, beyond this theoretical spectroscopy study, the calculations shed light into another interesting experimental feature studied by some of the authors of the present work. May *et al.*[6] observed the occurrence of delayed ionization and delayed emission of V^+ and Ti^+ ions following multiphoton absorption by the Ti and V met-cars. Based on an early calculation of the optical spectrum by Rubio *et al.*,[24] May *et al.* interpreted their experimental results as due to the excitation of a collective plasmon that later decays by emission of atomic ions. Our early calculation of the optical spectrum[24] used the TDDFT and a very simple model for the structure of the met-car, in which the effective potential seen by the valence electrons was spherically averaged about the center of the cluster.[25] This was a drastic approximation, later improved in a paper where we calculated the excitation spectrum of Ti_8C_{12} and V_8C_{12} met-cars taking fully into account the geometrical structure of the clusters[26] the T_d structure was assumed in the calculations). The present calculations complement that work by considering several low lying isomers.

To our knowledge, excited electronic states of the met-cars have not been investigated in an exhaustive way by *ab initio* techniques, and we expect that these studies may help to the experimental elucidation of the structures and may shed additional light on the processes of delayed ionization and ion emission in met-cars.

II. METHOD

The theoretical foundations of the TDDFT, as well as the computational scheme, has been described in detail elsewhere;[21,27–32] here we only summarize the main points. We begin by calculating the ground-state electronic structure of the different Ti_8C_{12} isomeric structures. Then, the absorption spectrum has been calculated for each isomer by using the formalism developed by Casida,[29] which requires the previous ground-state calculation of occupied and unoccupied Kohn-Sham electronic states in order to construct the noninteracting response function. After that, each excitation peak is broadened by a Lorentzian profile to construct the absorption spectrum. This methodology is computationally different, but essentially equivalent to the real time propagation method, where the ground state is instantaneously perturbed and the time-dependent Kohn-Sham equations are propagated in time[32] to get the frequency-dependent absorption cross section.[26–28,32] For the exchange-correlation energy functional we have used the adiabatic local spin-density approximation (LSDA), with the Perdew-Wang parametrization[33] for correlation. Test calculations using the Perdew-Burke-Ernzerhof generalized gradient approximation[34] (GGA) provide very similar results. The adiabatic LSDA has been used successfully in the calculation of the optical spectrum of atoms[35] and clusters of the nontransition elements.[22,23,35–38] However, less experience exists for the case of atoms with *d* electrons and their clusters.[26]

The ion-electron interaction is modeled by replacing the ionic cores (the $1s^2$ heliumlike core of the C atoms and the $1s^22s^22p^63s^23p^6$ argonlike core of the Ti atoms) by norm-conserving pseudopotentials. The scheme of Troullier and Martins[39] has been chosen for the C atoms due to the smooth pseudopotentials generated and to the good results that these pseudopotentials yield for systems containing first-row elements. On the other hand, for the Ti atoms we have used the scheme of Hartwigsen *et al.*[40] validated previously for transition metal clusters.[26] This pseudopotential is built in such a way that is separable by construction, is optimal for integration on a real-space grid, is highly accurate, and, due to its analytic form, can be specified by a very small number of parameters.

We took, as initial isomeric structures for Ti_8C_{12} those given by Sobhy *et al.*,[19] belonging to the symmetry groups C_{2v}, C_{3v}, C_s, D_2, D_{2d}, D_{3d}, D^*_{3d}, and T_d. Starting from those structures we have performed structural optimizations using of the Broyden algorithm[41] with a convergence criterion of 10^{-3} hartree/bohr for the net forces on each atom. For the relaxations we employed the ABINIT package,[42] and no significant variations were noticed with respect to the starting structures. The optimized geometries then used for the calculation of the photoabsorption spectra are shown in Fig. 1; those are described in full detail in Refs. 13 and 19. Once the electronic ground-state structure of the different isomers was

TABLE I. Cohesive energies per atom and relative energies of the different Ti_8C_{12} structures. The magnetic moments, Fermi level energies, HOMO-LUMO gaps, and static polarizabilities are also given.

	C_{3v}	T_d	C_{2v}	C_s	D_{2d}	D_2	D_{3d}^*	D_{3d}
Cohesive energy per atom (eV)	8.36	8.33	8.32	8.31	8.26	8.24	8.21	8.20
ΔE with respect to C_{3v} (eV)	0	0.67	0.83	1.05	2.05	2.40	3.07	3.15
Magnetic moment (μ_B)	2	2	0	0	0	0	2	2
Fermi level energy (eV)	−3.18	−3.42	−3.77	−4.10	−3.80	−3.88	−3.93	−3.98
HOMO-LUMO gap (eV)	0.26	0	0.72	0.52	0.59	0.36	0.36	0
Static polarizability (Å^3)	60.11	56.81	59.59	58.02	59.70	60.39	58.47	57.25

established, we performed the calculation of the photoabsorption spectrum with the OCTOPUS code.[27] The main numerical parameters that need to be specified are the following: the spacing of the spatial mesh, 0.2 Å, the wave function domain, a sphere of radius 8.5 Å, and the number of unoccupied states for the calculation of the excitations by the Casida formula[29] (the whole set of 40 occupied states and 40–50 unoccupied states have been necessary to reach convergence of the spectra for excitation energies up to 15 eV).

III. RESULTS

A. Ground-state properties

The cohesive energies per atom of the Ti_8C_{12} isomers of Fig. 1, and the relative energies with respect to the C_{3v} equilibrium configuration, are reported in Table I. The table also shows the net magnetic moments, Fermi level energies, highest occupied molecular orbital-lowest unoccupied molecular orbital (HOMO-LUMO) gaps, and the static polarizabilities. The cohesive energies per atom have been obtained from the expression

$$E_c/\text{atom} = \frac{E_t(\text{Ti}_8\text{C}_{12}) - [8E_t(\text{Ti}) + 12E_t(\text{C})]}{20}, \quad (1)$$

where $E_t(Ti_8C_{12})$, $E_t(Ti)$, and $E_t(C)$ are total energies of the cluster and the free atoms, respectively. The most stable structure is the C_{3v}, in agreement with the most recent calculations.[19] The cohesive energies of the different isomers are rather similar (the differences between the four most stable isomers are smaller than 0.05 eV, or 580 K) and this explains the debate on the ground-state structure of met-cars. The C_{3v}, T_d, D_{3d}^*, and D_{3d} isomers are spin polarized, and have net magnetic moments of $2\mu_B$. The HOMO level shows double and triple degeneracy in the D_{3d} and T_d isomers, respectively, leading to the corresponding Jahn-Teller distorted D_{3d}^* and C_{3v} geometries. The HOMO-LUMO gaps vary between 0 and 0.7 eV. There is no HOMO-LUMO gap in the T_d and D_{3d} structures due to the multiple degeneracy of the HOMO.

The static dipole polarizability tensor $\boldsymbol{\alpha}$ relates, to first order, the polarization vector **P** to the applied electric field **E**. The averaged static dipole polarizability is obtained from the trace of the $\boldsymbol{\alpha}$ tensor as $\langle\alpha\rangle = \frac{1}{3}\text{Tr}(\boldsymbol{\alpha})$. The polarizability tensor has been obtained by applying a small static electric field along each of the three Cartesian directions, and calculating the polarization vector. The calculations were repeated for electric fields of different magnitude, to make sure that the applied field was small enough to ensure the linear relationship between **P** and **E** on the one hand, and at the same time large enough to minimize numerical errors. For all the isomers, the tensor is almost isotropic due to their high symmetry, and the averaged polarizabilities are very similar, with values between 4.5 and 5 Å^3/atom. The present results are in quite good agreement with previous calculations performed for some isomers only.[15,26] The polarizabilities of the met-car are of the same order of magnitude of the polarizabilities of transition metal clusters [the polarizability of V_4^+, for instance, is near 5 Å^3/atom (Ref. 44)], but lower than the polarizabilities of alkali metal clusters: for instance, the polarizability of Li_8 calculated by TDDFT (Ref. 43) is 12 Å^3/atom.

Several surfaces of constant charge density have been

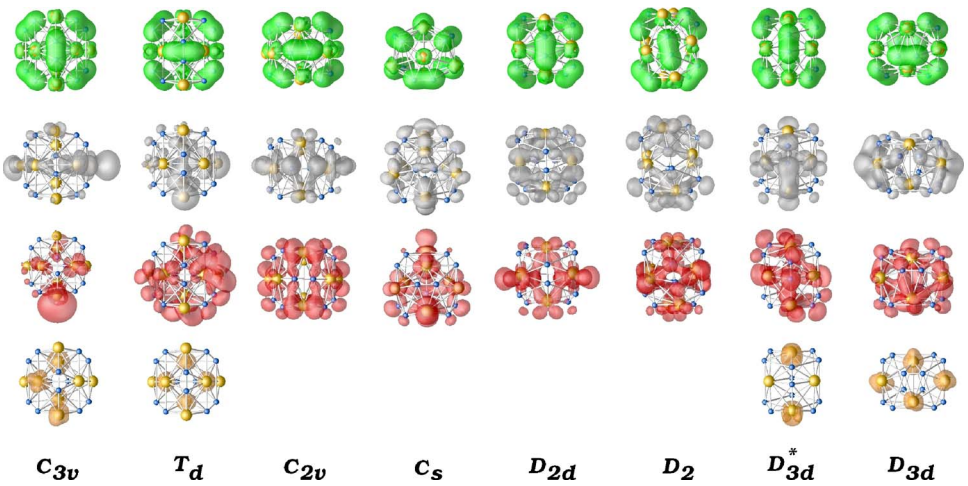

FIG. 2. (Color online) Surfaces of constant charge density for the different Ti_8C_{12} isomers of the Fig. 1. From top to bottom: (1) total charge density (0.1 e/a.u.^{3}) isosurface; (2) HOMO charge density (0.001 e/a.u.^{3}) isosurface; (3) LUMO charge density (0.001 e/a.u.^{3}) isosurface; (4) spin polarized charge density (0.02 e/a.u.^{3}) isosurface for the C_{3v}, T_d, D_{3d}^*, and D_{3d} structures.

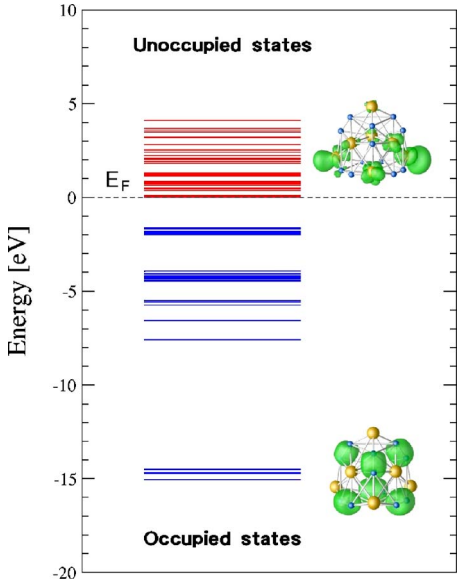

FIG. 3. (Color online) Kohn-Sham electronic energy levels for the ground-state Ti_8C_{12} met-car structure. The Fermi energy is taken as the zero energy reference. Surfaces of constant density corresponding to a strongly bound electronic state and to a low lying unoccupied state are also plotted.

plotted in Fig. 2 for the different Ti_8C_{12} isomers. From top to bottom: (1) the total charge density, $\rho_{\text{tot}}(\mathbf{r})=\rho_{\uparrow}(\mathbf{r})+\rho_{\downarrow}(\mathbf{r})$, where $\rho_{\uparrow}$ and $\rho_{\downarrow}$ are the spin up and spin down charge densities, respectively; (2) the charge density of the HOMO level, $\rho_{\text{HOMO}}(\mathbf{r})=|\psi_{\text{HOMO}}(\mathbf{r})|^2$; (3) the charge density of the LUMO level, $\rho_{\text{LUMO}}(\mathbf{r})=|\psi_{\text{LUMO}}(\mathbf{r})|^2$; and (4) for the C_{3v}, D_{3d}, D_{3d}^*, and T_d structures, the spin-polarized charge density, or spin magnetization, $\rho_{\text{spin}}(\mathbf{r})=m(\mathbf{r})=\rho_{\uparrow}(\mathbf{r})-\rho_{\downarrow}(\mathbf{r})$. The values of the different isosurfaces have been chosen for an optimal visualization. The particular magnitudes of those isosurfaces are indicated in the caption of Fig. 2. The electronic charge density on the Ti atoms is directly proportional to their coordination number (the same conclusion was extracted from a previous study of Sobhy *et al.*[19]), while the magnetization becomes noticeable in the Ti atoms with a lower coordination. $\rho_{\text{tot}}(\mathbf{r})$ also reaches high values around the C_2 units. It is valuable to appreciate how the symmetry of the isosurfaces is modified for the Jahn-Teller forms C_{3v} and D_{3d}^* with respect to their T_d and D_{3d} analogs; in particular, for the magnetization of the C_{3v} structure, where the specular symmetry is broken.

The Kohn-Sham orbital energies for the electronic ground state of the C_{3v} structure are given in Fig. 3. Both occupied and unoccupied states are included and the energy zero is taken at the Fermi level. The tightly bunched group of strongly bound occupied states detached from the rest corresponds to orbitals localized on the carbon dimers. A surface of constant density corresponding to one of those orbitals is plotted in the figure. The other occupied states, with smaller binding energies, have orbitals with a more complex spatial shape and a higher degree of delocalization though the cluster. Many of the low lying unoccupied states are localized near the Ti atoms and a representative member of those orbitals is also plotted.

B. Photoabsorption spectrum

Figures 4 and 5 show the photoabsorption cross sections for the ground state and the low lying isomers of Ti_8C_{12}, as obtained by the TDDFT calculation. Due to (a) the evident differences between the absorption spectra at low energies, and (b) our interest in the characteristic photoabsorption be-

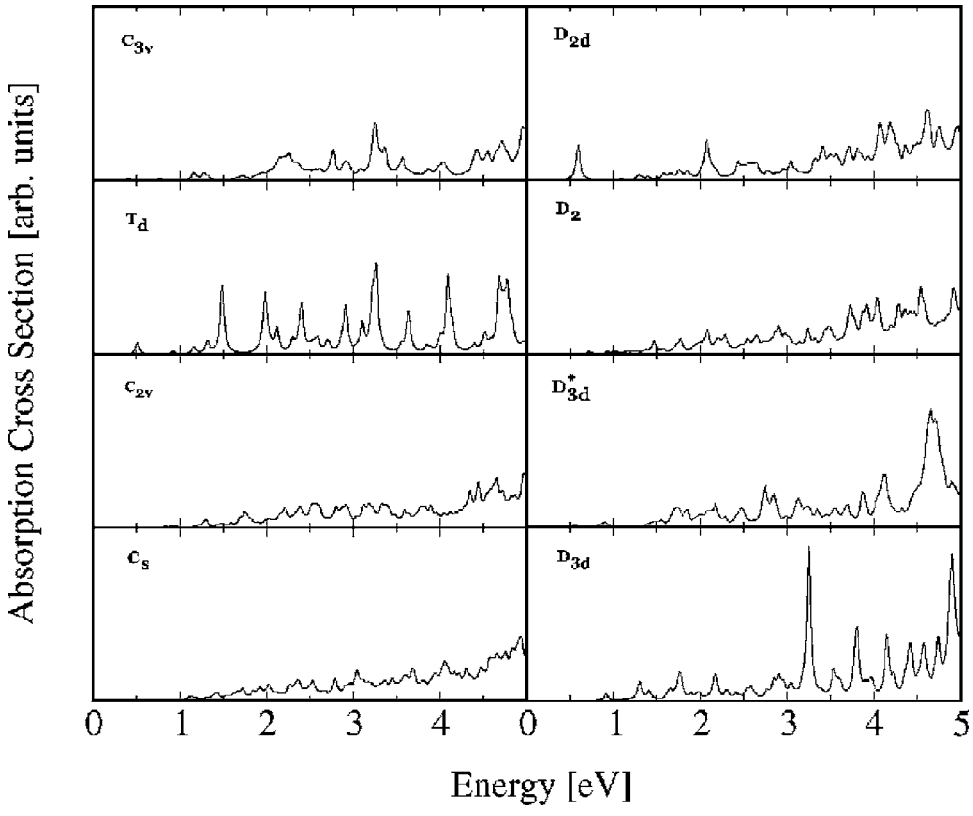

FIG. 4. Photoabsorption cross section (in arbitrary units) of the ground state (C_{3v}) and low lying isomers (T_d, C_{2v}, C_s, D_{2d}, D_2, D_{3d}^*, and D_{3d}) of Ti_8C_{12}, up to 5 eV.

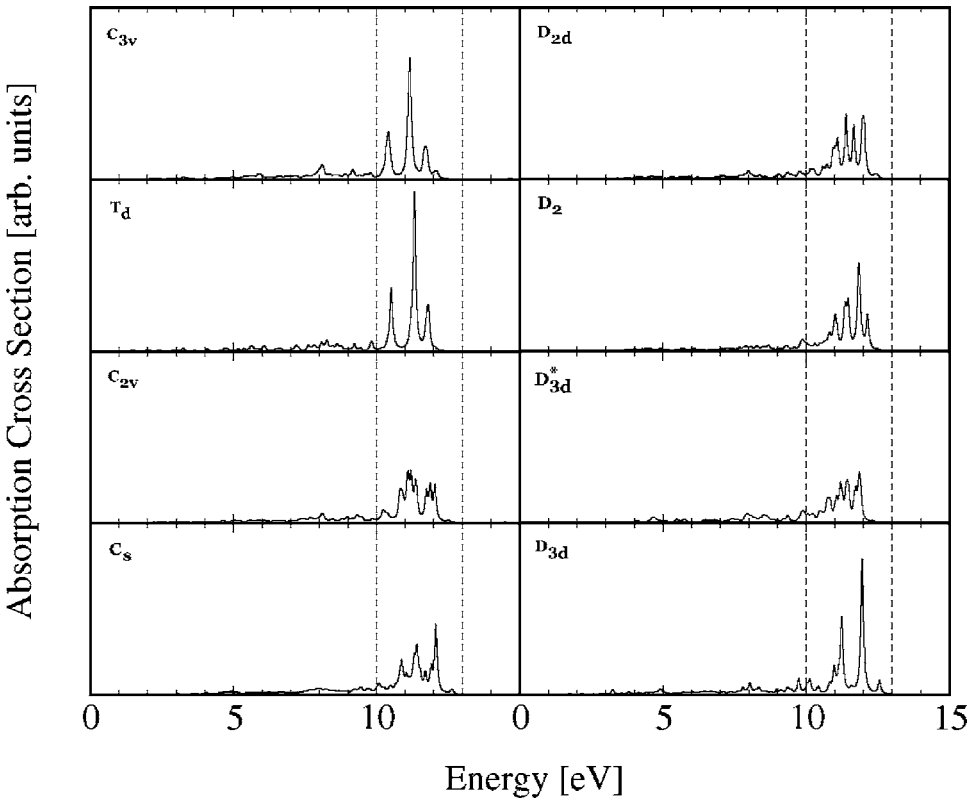

FIG. 5. Photoabsorption cross section (in arbitrary units) of the ground state (C_{3v}) and low lying isomers (T_d, C_{2v}, C_s, D_{2d}, D_2, D^*_{3d}, and D_{3d}) of Ti_8C_{12}, up to 15 eV. The vertical dashed lines delimit the collective plasmon region between 10–13 eV. Notice the different scale for the spectra with respect to Fig. 4.

havior of the met-cars at high energies, we show the two regions separately in Figs. 4 and 5. The finite width of the absorption peaks in an experimental spectrum—linked to the accessible resolution—is mostly determined by the temperature. In our calculations, on the other hand, each excitation peak in the spectrum has been broadened by a Lorentzian,

$$\sigma_{\text{absorption}}(\epsilon) = \sum_{\epsilon_i} \frac{A^2}{(\epsilon - \epsilon_i)^2 + A^2}. \tag{2}$$

In this equation ϵ is the energy, ϵ_i are the discrete excitation energies obtained by the Casida formula,[29] and the value of the parameter A, which determines the full width at half maximum (FWHM=2A) of the peaks, is set equal to 0.001 a.u. in Fig. 4 and equal to 0.002 a.u. in Fig. 5 respectively, which are values commonly used in order to mimic the experimental resolution.

The low energy spectra of Fig. 4, although weak in strength, are very rich and display clear differences between the different isomers. Weak low energy peaks are present near 0.5 eV in the D_{2d} and T_d isomers, and at 0.8 eV in the D_{3d} and the D^*_{3d} isomers. More generally, all the structures show a trend of increasing absorption cross section starting at an energy of 1 eV. The spectra of the T_d and the D_{3d} isomers show sharp excitation peaks between 1 and 5 eV. These distinct features are due to the high symmetry of those two clusters. In fact, the other spectra do not present such distinct absorption peaks. In particular, the C_{2v}, C_s, and D_2 isomers have a smoother and lower absorption profile than the more symmetric ones. All isomers show significant absorption in the region 4.5–5 eV. The ground-state C_{3v} structure presents its most characteristic absorption features in the region between 2 and 3.5 eV. Since clear differences have been established among the spectra of the different isomers in the low energy region (0–5 eV), we propose that a comparison of future experimental measurements to these TD-DFT spectra can serve as a tool to elucidate between the different isomeric forms and possibly confirm the C_{3v} structure as the ground state.

Figure 5 shows the photoabsorption spectra for the full range of energies, up to 15 eV. Two regions can be distinguished in all the spectra: a weak absorption profile covers the energy region up to 10 eV, and a region of strong absorption occurs at high energies between 10 and 13 eV. This region is delimited by the vertical dashed lines in Fig. 5. The profile of the spectrum in this high energy region varies somehow from cluster to cluster, although there are similarities between the spectra of the C_{3v}, T_d, and D_{3d} isomers, and between the spectra of the D_2 and D_{2d} isomers. But in all cases this broad region of high absorption can be interpreted as due to strong and complex electronic excitations qualitatively similar for all the isomers studied. Those are excitations from the bunch of states lying approximately 15 eV below the Fermi level (the orbitals of those states, as indicated at the end of Sec. III A above, are localized on the C_2 bonds) to low lying unoccupied states above the Fermi energy, and have a collective character. Electronic screening lowers the energy of the unscreened transitions, leading to high absorption strength in the 10–13 eV range. We did not find significant variations in the form of the absorption spectrum in this high energy region by using additional unoccupied states for the calculation of the excitations and this indicates that the results are well converged. The structure of the collective excitations is more fragmented for the isomers

with higher symmetry, that is, the C_{3v}, D_{3d}, and T_d isomers. The less symmetric structures present a smoother absorption profile.

We now relate the results of our calculations of the photoabsorption spectrum to experiments where May *et al.*[6] observed delayed ionization (DI) and delayed ion emission (DIE) in the Ti and V met-cars. A necessary condition for DI to occur is that the ionization potential has to be smaller than the dissociation energy of the cluster. In such a case, competition between prompt ionization and dissociation may lead to delayed ionization. This condition is met in met-cars. Our calculations for Ti_8C_{12} give a cohesive energy slightly above 8 eV/atom (see Table I). Other calculations of the binding energies of the Ti_8C_{12} give E_b=6.62 eV/atom (Ref. 45) and 6.54 eV/atom,[12] and collision-induced dissociation experiments give an upper limit of 9 eV for the dissociation threshold.[46] All those values are larger than the calculated ionization potential of Ti_8C_{12}, which is about 5.2 eV. [26] In addition to this requirement, the cluster must generate its own "heat bath" allowing to store the excitation energy in a broad region of closely spaced excited states centered at an energy close to the sum of the dissociation energy of the cluster and the ionization potential of the metal atom. This places that region around 12–13 eV for the Ti met-car. The results given in Fig. 5 show indeed a broad absorption region that begins near 10 eV and has maximum strength around 12–13 eV, giving support to the original interpretation of the experiment.[6] According to the calculated spectra, the energy range for the region of collective excitations is a robust characteristic of the Ti_8C_{12} met-car, not affected by the precise geometry of the isomer. Then, one can guess confidently that the existence of a broad energy region of strong collective excitations is a characteristic of the met-cars.

IV. CONCLUSIONS

The ground-state structure of Ti_8C_{12} and related metallocarbohedrynes has been a subject of debate in the recent literature. Using the TDDFT formalism we have calculated the photoabsorption spectra of the most stable isomers of Ti_8C_{12} for energies up to 15 eV. Substantial differences are found between the absorption spectra in the low energy region (0–5 eV), and we conclude that a comparison between the calculated photoabsorption spectra and future measurements could be used to elucidate between the different structures proposed from theoretical total energy calculations by different authors. The spectrum of all the isomers presents a region of high absorption between 10 and 13 eV. We interpret the high absorption as due to the excitation of collective electronic modes. This high energy absorption feature has been previously observed in the experiments of May *et al.*[6] It provides an internal heat bath that allows to explain the occurrence of delayed ionization and delayed ion emission from these metallocarbohedrynes.

ACKNOWLEDGMENTS

This work was supported by MEC of Spain (Grant No. MAT2005-06544-C03-01), Junta de Castilla y León (Grant No. VA039A05), and the EC 6th Framework Network od Excellence NANOQUANTA (NMP4-CT-2004-500198). One of the authors (J.I.M.) acknowledges support from the MEC under the FPI graduate fellowship program, and also the hospitality of the Institut für Theoretische Physik (Freie Universität Berlin). One of the authors (A.C.) acknowledges support from the Sonderforschungsbereich 450. One of the authors (A.R.) acknowledges the Humboldt Foundation under the Bessel award (2005). One of the authors (J.A.A.) acknowledges the hospitality and support of the Donostia International Physics Center (DICP). They are grateful to M. A. Sohby, A. W. Castleman, and J. Sofo, who kindly provided detailed information on the geometries of the met-car isomers, and for their interest in this work.

[1] B. C. Guo, K. P. Kerns, and A. W. Castleman, Jr., Science **255**, 1411 (1992); B. C. Guo, S. Wei, J. Purnell, S. Buzza, and A. W. Castleman, Jr., *ibid.* **256**, 515 (1992).
[2] B. C. Guo, K. P. Kerns, and A. W. Castleman, Jr., J. Am. Chem. Soc. **115**, 7415 (1993).
[3] S. Wei, B. C. Guo, J. Purnell, S. Buzza, and A. W. Castleman, Jr., J. Phys. Chem. **96**, 4166 (1992).
[4] S. Wei, B. C. Guo, J. Purnell, S. A. Buzza, and A. W. Castleman, Jr., Science **256**, 818 (1992); S. Wei, B. C. Guo, H. T. Deng, K. P. Kerns, J. Purnell, S. A. Buzza, and A. W. Castleman, Jr., J. Am. Chem. Soc. **116**, 4475 (1994).
[5] S. F. Cartier, B. D. May, and A. W. Castleman, J. Chem. Phys. **100**, 5384 (1994); S. F. Cartier, B. D. May, and A. W. Castleman, J. Am. Chem. Soc. **116**, 5295 (1994); B. C. Guo, H. T. Deng, K. P. Kerns, and A. W. Castleman, Int. J. Mass Spectrom. Ion Process. **138**, 275 (1994).
[6] B. D. May, S. F. Cartier, and A. W. Castleman, Chem. Phys. Lett. **242**, 265 (1995).
[7] P. Liu, J. A. Rodriguez, and J. T. Muckerman, J. Phys. Chem. B **108**, 18796 (2004).
[8] M. M. Rohmer, M. S. Bénard, and J. M. Poblet, Chem. Rev. (Washington, D.C.) **100**, 495 (2000).
[9] W. Kohn and L. J. Sham, Phys. Rev. **140**, A1133 (1965).
[10] I. Dance, J. Chem. Soc., Chem. Commun. **24**, 1779 (1992).
[11] I. Dance, J. Am. Chem. Soc. **118**, 6309 (1996).
[12] H. Chen, M. Feyereisen, X. P. Long, and G. Fitzgerald, Phys. Rev. Lett. **71**, 1732 (1993).
[13] M. M. Rohmer, M. S. Bénard, C. Henriet, C. Bo, and J. M. Poblet, J. Chem. Soc., Chem. Commun. **15**, 1182 (1993).
[14] M. M. Rohmer, M. S. Bénard, C. Bo, and J. M. Poblet, J. Am. Chem. Soc. **117**, 508 (1995); M. S. Bénard, M. M. Rohmer, J. M. Poblet, and C. Bo, J. Phys. Chem. **99**, 16913 (1995).
[15] G. K. Gueorguiev and J. M. Pacheco, Phys. Rev. Lett. **88**, 115504 (2002).
[16] H. Harris and I. Dance, J. Phys. Chem. A **105**, 3340 (2001).
[17] T. Baruah, M. R. Pederson, M. L. Lyn, and A. W. Castleman, Phys. Rev. A **66**, 053201 (2002).
[18] T. Baruah and M. R. Pederson, Phys. Rev. B **66**, 241404 (2002).
[19] M. A. Sohby, A. W. Castleman, Jr., and J. O. Sofo, J. Chem. Phys. **123**, 154106 (2005).
[20] K. Deng, W. Duan, and B. Gu, J. Chem. Phys. **121**, 4123 (2004).
[21] E. Runge and E. K. U. Gross, Phys. Rev. Lett. **52**, 997 (1984); E. K. U. Gross, J. F. Dobson, and M. Petersilka, in *Topics in Current Chemistry*, edited by R. F. Nalewajski (Springer, Heidelberg, 1996), Vol. 81, p. 81; G. Onida, L. Reining, and A. Rubio, Rev. Mod. Phys. **74**, 601 (2002); M. A. L. Marques and E. K. U. Gross, in *A Primer in Density Functional Theory*, edited by C. Fiolhais, F. Nogueira, and M. A. L. Marques (Springer, Berlin, 2003), p. 144.
[22] A. Rubio, J. A. Alonso, X. Blase, L. C. Balbás, and S. G. Louie, Phys. Rev. Lett. **77**, 247 (1996).
[23] A. Castro, M. A. L. Marques, J. A. Alonso, G. F. Bertsch, K. Yabana, and A. Rubio, J. Chem. Phys. **116**, 1930 (2002).
[24] A. Rubio, J. A. Alonso, and J. M. López, An. Fis. **89**, 174 (1993).
[25] M. P. Iñiguez, M. J. López, J. A. Alonso, and J. M. Soler, Z. Phys. D: At., Mol. Clusters **11**, 163 (1989).
[26] J. I. Martínez, A. Castro, A. Rubio, J. M. Poblet, and J. A. Alonso, Chem. Phys. Lett. **398**, 292 (2004).
[27] M. A. L. Marques, A. Castro, G. F. Bertsch, and A. Rubio, Comput. Phys.

Commun. **151**, 60 (2003); A. Castro, H. Appel, M. Oliveira, C. A. Rozzi, X. Andrade, F. Lorenzen, E. K. U. Gross, M. A. L. Marques, and A. Rubio, Phys. Status Solidi B **243**, 2465 (2006).
[28] K. Yabana and G. F. Bertsch, Phys. Rev. B **54**, 4484 (1996); Phys. Rev. A **60**, 1271 (1999); **60**, 3809 (1999); Int. J. Quantum Chem. **75**, 55 (1999).
[29] M. E. Casida, in *Recent Advances in Density Functional Methods, Part I*, edited by D. P. Chong (World Scientific, Singapore, 1995), p. 155.
[30] C. Jamorski, M. E. Casida, and D. R. Salahub, J. Chem. Phys. **104**, 5134 (1996).
[31] M. Petersilka, U. J. Gossmann, and E. K. U. Gross, Phys. Rev. Lett. **76**, 1212 (1996).
[32] A. Castro, M. A. L. Marques, and A. Rubio, J. Chem. Phys. **121**, 3425 (2004).
[33] J. P. Perdew and Y. Wang, Phys. Rev. B **45**, 13244 (1992).
[34] J. P. Perdew, K. Burke, and M. Ernzerhof, Phys. Rev. Lett. **77**, 3865 (1996); **78**, 1396 (1997).
[35] I. Vasiliev, S. Ogut, and J. R. Chelikowsky, Phys. Rev. Lett. **82**, 1919 (1999).
[36] A. Rubio, J. A. Alonso, X. Blase, and S. G. Louie, Int. J. Mod. Phys. B **11**, 2727 (1997).
[37] M. A. L. Marques, A. Castro, and A. Rubio, J. Chem. Phys. **115**, 3006 (2001).
[38] D. Tsolakidis, D. Sánchez-Porta, and R. M. Martin, Phys. Rev. B **66**, 235416 (2002).
[39] N. Troullier and J. L. Martins, Phys. Rev. B **43**, 1993 (1991).
[40] C. Hartwigsen, S. Goedecker, and J. Hutter, Phys. Rev. B **58**, 3641 (1998).
[41] C. G. Broyden, Math. Comput. **19**, 577 (1965).
[42] X. Gonze, J. M. Beuken, R. Caracas *et al.*, Comput. Mater. Sci. **25**, 478 (2002); M. Fuchs and M. Scheffler, Comput. Phys. Commun. **119**, 67 (1999); The ABINIT code is a common project of Université Catholique de Louvain, Corning Incorporated, and other contributors (URL http://www.abinit.org).
[43] A. Castro, M. A. L. Marques, J. A. Alonso, and A. Rubio, J. Comput. Theor. Nanosci. **1**, 231 (2004).
[44] J. I. Martínez, A. Castro, A. Rubio, and J. A. Alonso, J. Comput. Theor. Nanosci. (to be published).
[45] B. V. Reddy, S. N. Khanna, and P. Jena, Science **258**, 1640 (1992).
[46] K. P. Kerns, B. C. Guo, H. T. Deng, and A. W. Castleman, Chem. Phys. Lett. **198**, 118 (1992).